ADVANCED FUNCTIONAL MATERIALS
www.afm-journal.de

Influence of Direct Laser Written 3D Topographies on Proliferation and Differentiation of Osteoblast-Like Cells: Towards Improved Implant Surfaces

Judith K. Hohmann and Georg von Freymann*

The influence of truly three-dimensional microstructures on osteoblast-like cells is reported. Well defined templates are fabricated by direct laser writing and biocompatibly coated with titanium dioxide, resembling implant surfaces. The influence of structural parameters on proliferation, morphology, adhesion, and differentiation is studied. A significantly higher proliferation (170%) is observed on particular topographies compared to unstructured surfaces. Additionally, an influence of structural parameters on the morphology of osteoblast-like cells is obtained, whereas all cells possess the osteoblastic marker alkaline phosphatase within all structures.

1. Introduction

With society growing older, implants are often necessary to preserve mobility and health-related quality of life. The surgical intervention of implantation is routinely done by skilled physicians, who have access to highly developed technologies and materials.

However, dental implant failure occurs in up to eight percent, usually resulting from deficit osseointegration or insufficient adaptation of soft tissue.[1] Many approaches to improve dental implant acceptance deal with chemical and/or physical surface treatments (e.g., acid-etching or sand-blasting[2–4] leading to randomly shaped, 2.5D patterns. It was shown that these surface treatments have an influence on proliferation of cells,[7–9] but the underlying reasons are poorly understood.[10] To obtain a better understanding of cell-surface interaction, it is important to systematically study the physical influence. Patterns fabricated by acid-etching or sand-blasting lack truly three- dimensional motifs with defined sizes. Systematic studies with freely chosen parameter variations are hardly possible with these surface treatments and consequently rarely conducted.[11,12]

J. K. Hohmann, Prof. G. von Freymann
Physics Department and Research Center OPTIMAS
University of Kaiserslautern
67663, Kaiserslautern, Germany
E-mail: jhohmann@physik.uni-kl.de
Prof. G. von Freymann
Fraunhofer Institute for Physical
Measurement Techniques IPM
Department of Materials Characterization and Testing
Erwin-Schroedinger-Str., Building 56, 67663, Kaiserslautern, Germany

DOI: 10.1002/adfm.201401390

With different fabrication techniques, which are not used for dental implants (e.g., mask lithography, injection molding), it is possible to produce 2.5D topographies with defined sizes. It was shown that these topographies are able to influence differentiation,[13–15] proliferation[16] and morphology[17,18] of different cells. Nevertheless, results generated in two-dimensional systems can hardly be transferred to natural, three-dimensional systems.[5,6]

For the design of ultimately improved implant materials, it is therefore necessary to develop surfaces with controlled and standardized three-dimensional topographies.[10]

Additionally, it is mandatory to exclude chemical influence on cells through different materials or inhomogeneous nutrient supply since it is known that these parameters influence cell growth as well.[19,20] By eliminating chemical inhomogeneity it is possible to clearly study whether and how cellular behavior is changed within different topographies.

Here, we report the first systematic study of the influence of truly three-dimensional topographies with chemically homogeneous surfaces on viability parameters of osteoblast-like cells. Using direct laser writing, we are able to reproducibly fabricate well-defined, three-dimensional structures consisting of polymer material (see experimental section for details). To exclude chemical influences of substrate biochemistry and to ensure biocompatibility[21–23] we coat the structures with TiO_2 resulting in a surface chemistry found on most implants: Titanium with its native oxygen layer is a widely accepted implant material.[10] To uniformly coat both the three-dimensional structures and the substrate, we use atomic layer deposition (ALD). Even coating of porous material is possible since gas phase precursors are used, making ALD the method of choice over other techniques like electron beam evaporation or sputtering.[24] Differently to other studies of the influence of cell shape on cellular behavior,[13,17,18,25,26] we do not coat selected topographic features with proteins like fibronectin to enhance cellular adhesion and simultaneously force the cells to a certain shape.

Along these lines we are able to observe how cells react only to differences in topographic parameters, e.g., different lattice spacing or square and hexagonal arrangement of topographical features. The observations derived by systematic variations might pave the way to understand the physical cues of topography-cell interaction. Enhanced proliferation due to these

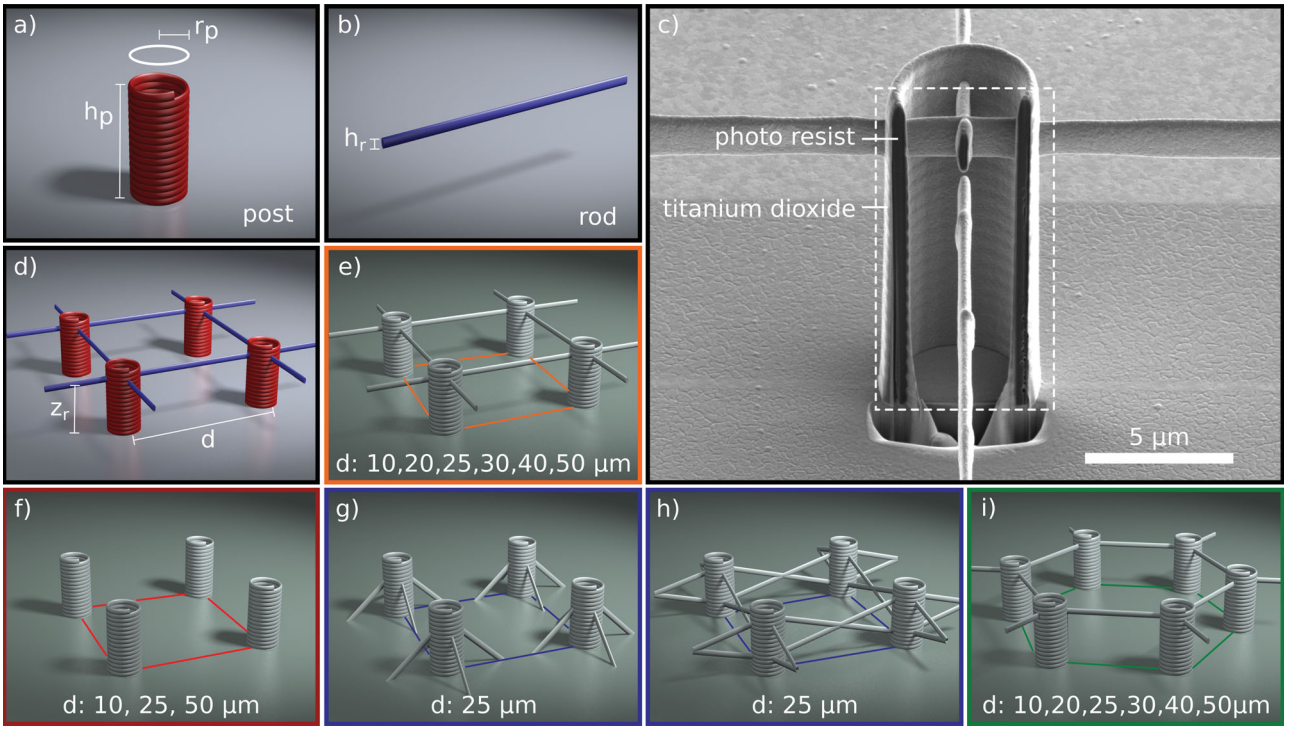

Figure 1. Overview of fabricated samples. All topographies are built using only two basic elements namely a) hollow posts ($h_p = 12$ µm, $r_p = 5$ µm) and b) thin rods (ellipsoidal shape, major axis $h_r = 1.5$ µm, minor axis 0.45 µm due to the aspect ratio of the focal volume). d) These basic elements are arranged on different grids (e.g., square grid, $z_r = 10$ µm) and e) both structure and cover slip are coated with 50 nm titanium dioxide. For a focused ion beam cross section (highlighted as guide to the eye) of a post see (c). Four different structure sets are fabricated: f) posts on a square grid with variation of the post distance *d* and without connection, e) posts on a square grid connected with horizontal rods and variation of the post distance *d*, g) posts on a square grid with diagonal rods or h) with fence like rods and i) posts on a hexagonal grid connected with horizontal rods and variation of the post distance *d*. Compartments are highlighted (e–i).

topographies might on the long run guide the design of novel implants with decreased implant failure rates, if osteoblastic functionality is simultaneously secured by the structures.

2. Results and Discussion

For the experiments we systematically study different structures: Each sample covers an area of 500 µm × 500 µm. For an overview, see **Figure 1**. To ensure that cells feel a chemically constant environment, polymer and glass substrate are uniformly coated with a thin layer (50 nm) of titanium dioxide via ALD (Figure 1c). Samples are built using only two different basic elements: Solid posts (Figure 1a) and thin rods (Figure 1b). The thickness of the rods allows the cell to make focal adhesion contacts to the rods[27] and use them as guides.

We expect osteoblast-like cells to be not able to highly deform their nucleus, because it is much stiffer than the cell matrix.[28] Typical diameters of cell nuclei are in the range of 10 µm,[29] hence smallest post distances are chosen to be 10 µm. Since we observe a cell surface area of 2000 µm^2 on plain surfaces,[29] cells are not expected to span distances between rods or posts larger than 40–50 µm. Consequently, the upper distance limit is selected to be 50 µm. For some samples the posts are connected via rods (Figure 1e,h,i) to study whether cell-guiding is important. Different rod arrangements allow us to evaluate the influence of guiding. Furthermore, arrangements of posts as square grids are compared to hexagonal grids, because we expect that having more contact opportunities within one compartment positively influences proliferation. The combination of the different topographical variations results in four different sets of samples.

2.1. Fabricated Structures: Four Different Sample Sets

The first set consists of square grids (Figure 1f) built by posts which are not connected with rods. With this set we want to prove whether 3D features are necessary or if the spatial spacing of the posts is sufficient for cell guiding and to influence the proliferation of osteoblast-like cells.

The second set of structures arranges posts in a square grid and connects nearest neighbors with rods (**Figure** 1e, **2**a,d). In this experiment, we are interested in the influence of the post distance on the morphology and guiding of osteoblast-like cells, especially, which post distances are bridged by the cell without forming focal adhesion contacts to the substrate.

For the third set, we fabricate structures with different rod arrangements to prove whether this influences cell morphology and proliferation. The posts are spaced 25 µm apart in all structured fields, while the rods are built horizontally (Figure 1e), diagonally (so called bungee-like structure

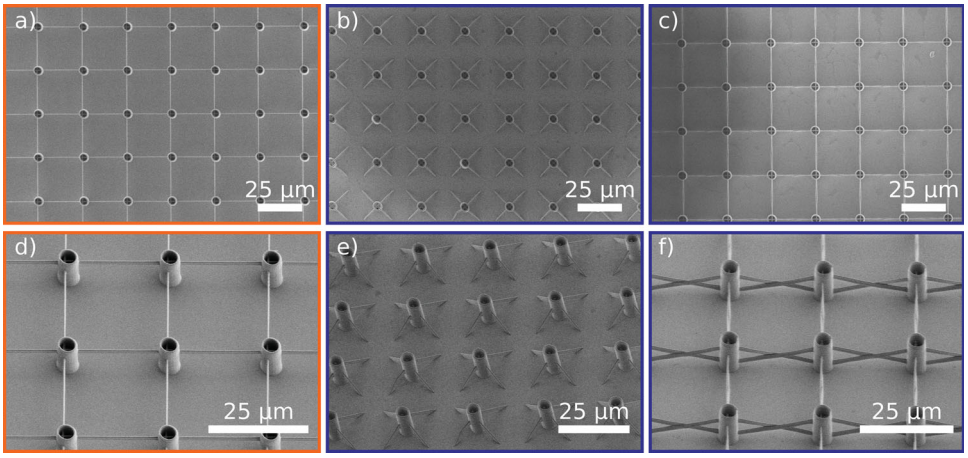

Figure 2. Scanning electron micrographs of different rod geometries with 25 µm spaced posts. Namely, a,d) square grids, b,e) bungee structures, and c,f) fence structures. a–c) Top view, d–f) tilted sample.

like shown in Figure 1g, 2b,e), or like a trellis-work fence (Figure 1h, 2c,f). Within the square grids, the rods are expected to lead the cell to other posts, where it can form more focal adhesion contacts due to a greater surface area of the posts compared to the rods. In the bungee-like structures cells should not be guided to other posts and in fence-like structures the geometry is expected to confine the cell within four posts.

With the fourth set of structures the influence of the structures on cell shape is studied. Therefore we fabricate hexagonal grids with equal post distances compared to the square grids, but 6 versus 4 posts within one compartment (**Figure 3**).

2.2. Proliferation

To study proliferation cells are counted every 24 h, beginning with 24 h after seeding. Within the first experiment, the influence of 2.5D structures on the proliferation rate of osteoblast-like cells is studied. Thereby, the post distance seems to have nearly no influence on the proliferation rate (**Figure 4**a). Proliferation rates of the cells on 10 µm spaced 2.5D posts that are not connected with rods are significantly smaller than on a 2D plain surface. Increasing the post distance has a very small effect on proliferation. This might be in contrast to the study by Unadkat et al.,[16] observing that cell proliferation can be influenced by a certain spatial distribution. Unfortunately, they did not report which spatial distribution enhances proliferation. One reason for the different results might be that they used only 5 µm high 2.5D structures with other shapes and another cell type.

If the structures are connected with horizontal posts, they have a greater influence on the proliferation (Figure 4b). In general, these structured areas seem to enhance proliferation, except 10 µm spaced posts where proliferation is significantly lower than on plain surfaces (Figure 4b). Statistic evaluation with Welch's *t*-test shows a significantly ($p < 0.001$) higher proliferation (136%) on 25 µm spaced posts than on 10 µm, 40 µm, 50 µm and on plain surfaces. The difference between 25 µm on the one hand and 20 µm or 30 µm on the other hand is also significant with $p < 0.01$. For 40 µm and 50 µm spaced posts we obtain no significant difference concerning proliferation compared to plain surfaces, because the cells are hardly able to

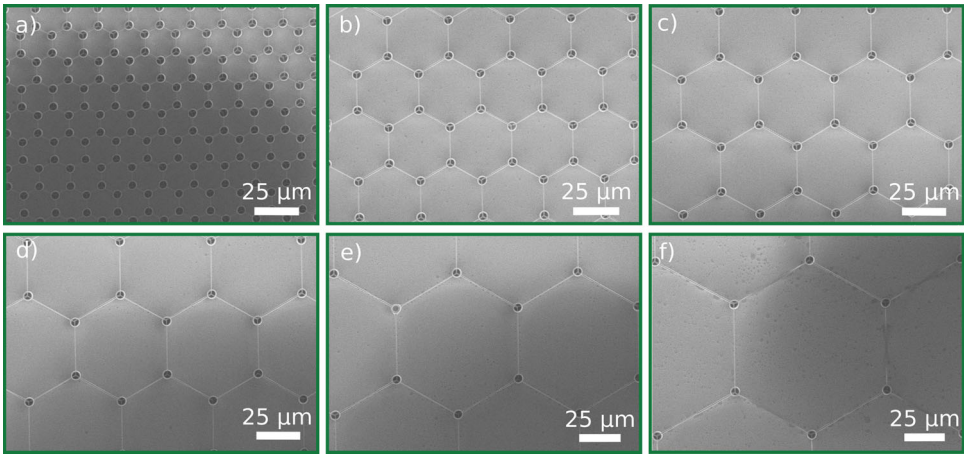

Figure 3. Scanning electron micrographs (top view) of hexagonal grid structure with different post distances: a) 10 µm, b) 20 µm, c) 25 µm, d) 30 µm, e) 40 µm, f) 50 µm.

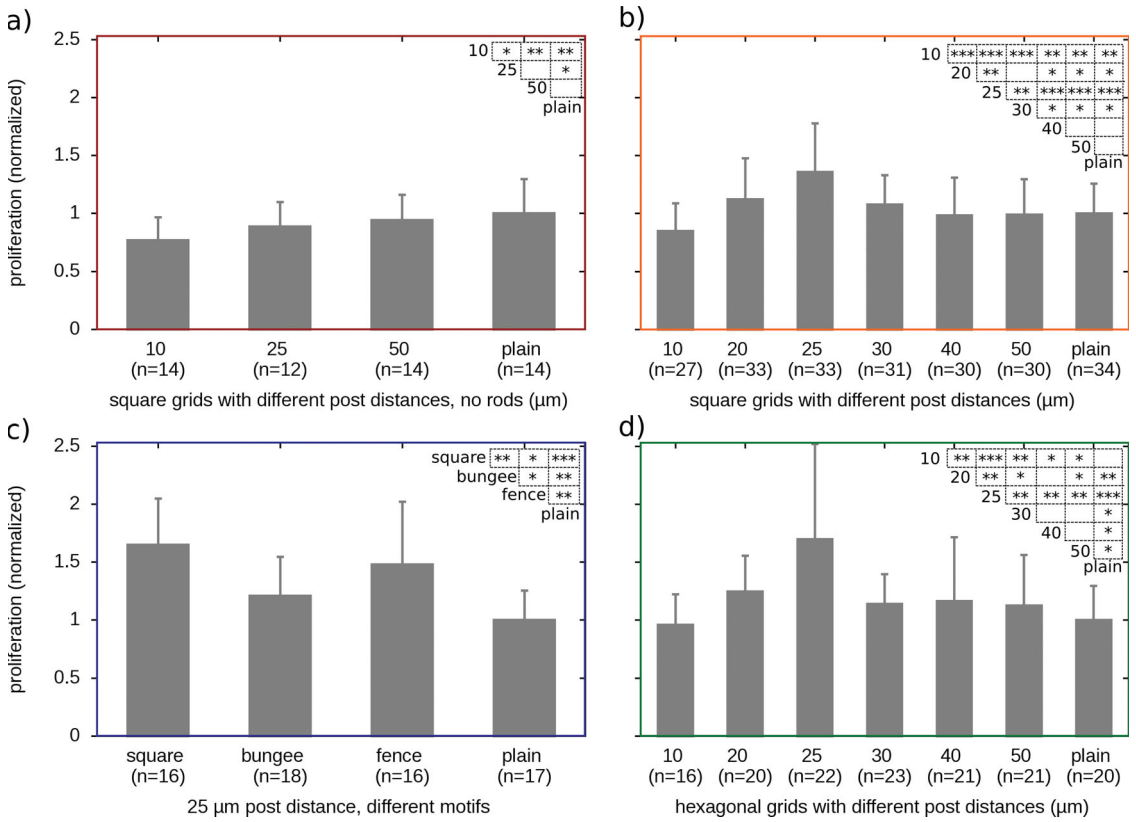

Figure 4. Proliferation within 48 h of SaOs-2 cells on the four different sets (a–d), mean value of *n* experiments is normalized to plain structures. Error bars indicate standard deviation, insets show p-values of Welch's *t*-test between every combination of structure with * for $p < 0.05$, ** for $p < 0.01$ and *** for $p < 0.001$. a) Proliferation on square grids without rods, b) variation of post distance on square grids, connected with horizontal rods. For example, proliferation on 25 µm spaced rods is significantly higher than on plain surfaces ($p < 0.001$) and on other post distances ($p < 0.01$ for 20 µm and 30 µm or even $p < 0.001$ for 10 µm, 40 µm, and 50 µm). Furthermore, proliferation c) 25 µm spaced rods with different rod geometries and d) on hexagonal grids.

span between the posts and therefore feel nearly the same topography as cells on plain surfaces. The differences concerning proliferation within connected vs not connected compartments support the hypothesis that cell guiding via rods has an effect on cellular behavior.

With the next experiment this is investigated further by varying the arrangements of the rods to bungee-like and fence-like structures (third set). This variation has a significant effect on proliferation, too. Precisely, square grids with horizontal rods show a significantly enhanced proliferation compared to fence-like and bungee-like structures and to plain surfaces (Figure 4c). Bungee rods are less effective concerning proliferation compared to square grids and fence-like structures, but still better than plain surfaces.

Furthermore, we are interested in whether the finding that proliferation is enhanced in 25 µm spaced posts connected with rods can be transferred to other grids with identical post distance and rod geometry. Posts arranged on a hexagonal grid (fourth set) provide the cell with 6 instead of 4 posts per compartment. Distances to bridge assisted by horizontal rods are kept constant but the surface area of a compartment is enhanced. We observe that proliferation of osteoblast-like cells is enhanced within 25 µm spaced posts (170%) and weakened in 10 µm spaced posts (Figure 4d). The trend of proliferation is similar to the square grids that are horizontally connected with rods.

All in all, posts that are spaced 25 µm apart from each other seem to enhance cell proliferation if they are connected via rods. Providing the cell with six instead of four reachable posts enhances proliferation, if post distance is kept constant. Post distances around 10 µm regardless of grid type suppress proliferation whereas large post distances show no significant difference concerning proliferation compared to plain surfaces.

2.3. Morphology and Adhesion Contacts

In order to study cell morphology the actin cytoskeleton, the nucleus and the focal adhesion contacts are fluorescently stained and observed with confocal laser scanning microscopy. Within the first set of parameters, cells show different behavior from structure to structure, but always interact with the templates: On 10 µm spaced posts, the majority of osteoblast-like cells has a long drawn-out cytoskeleton (**Figure 5**a–c) and is aligned parallel to the rods. The cells hardly grow into the structure (Figure 5a), but lie on top of the posts and rods (Figure 5c). Cell nuclei have an elliptical shape and align parallel to the rods. Similar cell morphology for another cell type (human lung

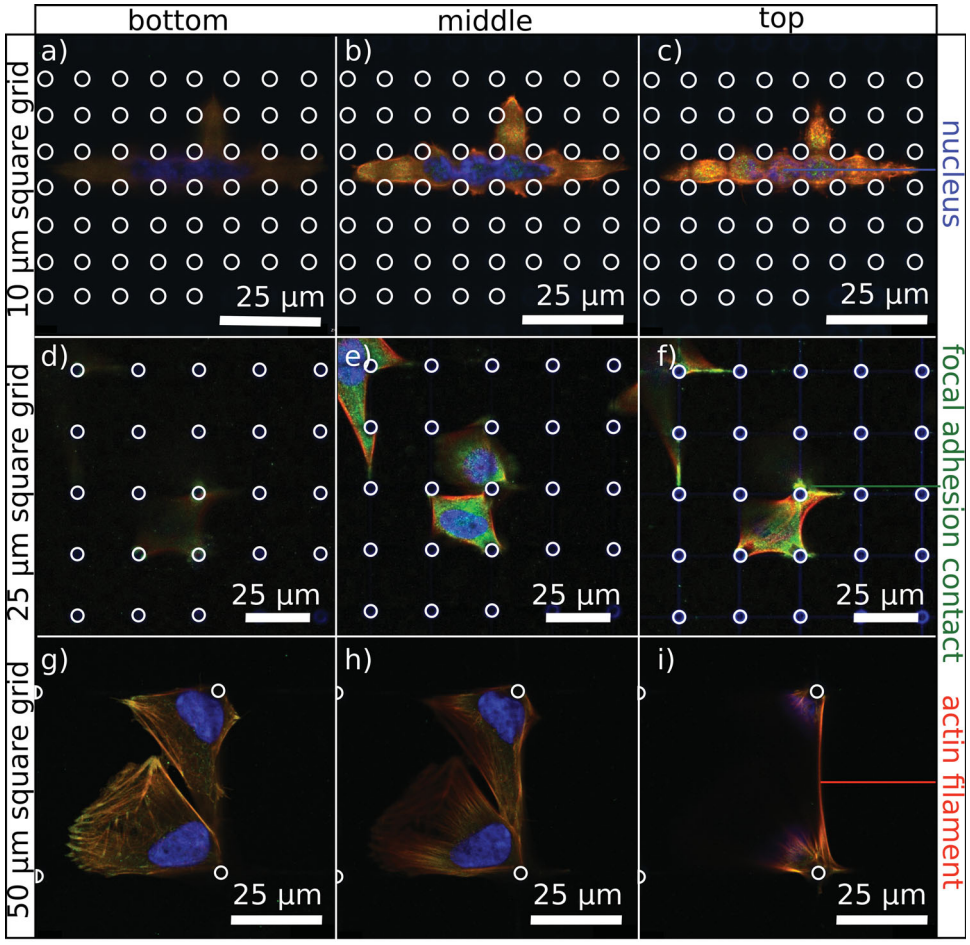

Figure 5. Confocal laser scanning micrographs of fluorescent stained cells on square grid structures (set 1) with different post distances. Actin (red), nucleus (blue) and focal adhesion contacts (green) are stained. Each column corresponds to a different z-layer of the samples (bottom, middle, top), each row to a different sample (10 µm (a–c), 25 µm (d–f), 50 µm square grid (g–i)). Structures are retraced white as a guide to the eye.

carcinoma cells A549) is observed by Greiner et al.[30] on a scaffold with 10 µm pore size. When spacing of the posts is increased, the long ellipsoidal axis of the cells becomes smaller. At 25 µm spaced post structures we often observe that the cells are suspended between four posts. They form focal adhesion contacts to both posts and rods and have rarely contact to the bottom (Figure 5d–f). For large post distances hardly any cell is able to make focal adhesion contacts to more than one post. Nevertheless, rods are often followed (Figure 5i). SaOs-2 cells mainly lie at the bottom of the structures showing a similar morphology like cells on plain surfaces. Surface area of the cell is larger than on 25 µm spaced posts, the cells grow mainly in *x*-*y*-direction.

The rod arrangement (third set) also influences cell morphology. On bungee like structures, cells seem to avoid the posts and rods (**Figure 6**a–c). They spread on the bottom of the structures, forming focal adhesion contacts to the substrate but rarely to the posts and rods (Figure 6a). The outer shape appears serrated. The underlying reason for this shape might be similar to the effect of gap guidance as described by Hamilton et al.[31] They observed that cells can be guided by discontinous-edge surfaces resulting in similar cell shapes as shown in Figure 6a–c.

Within the fence-like geometry, cells grow in one compartment (Figure 6d–f). They form focal adhesion contacts to 2–4 posts and their shape adapts to the structures. Within the compartment cells grow three-dimensionally into the structures, they often fill the whole compartment, but rarely expand above the rods. In hexagonal structures cells behave similarly to square grids. They form their cytoskeleton along the rods, building hexagonal or similar shapes when post distance is about 25 µm (Figure 6g–i) and are not able to bridge the post for larger post distances.

In summary, a similar morphology is achieved within 25 µm spaced square grids and 25 µm spaced hexagonal positioned posts both connected with horizontal rods, simultaneously we observe the highest proliferation within these grids.

2.4. Presence of Alkaline Phosphatase

To test whether the different structures do not prevent the function of the osteoblastic cells, namely to mineralize the extracellular matrix, we stain alkaline phosphates after 3 or 6 days growth of SaOs-2 cells within the three-dimensional

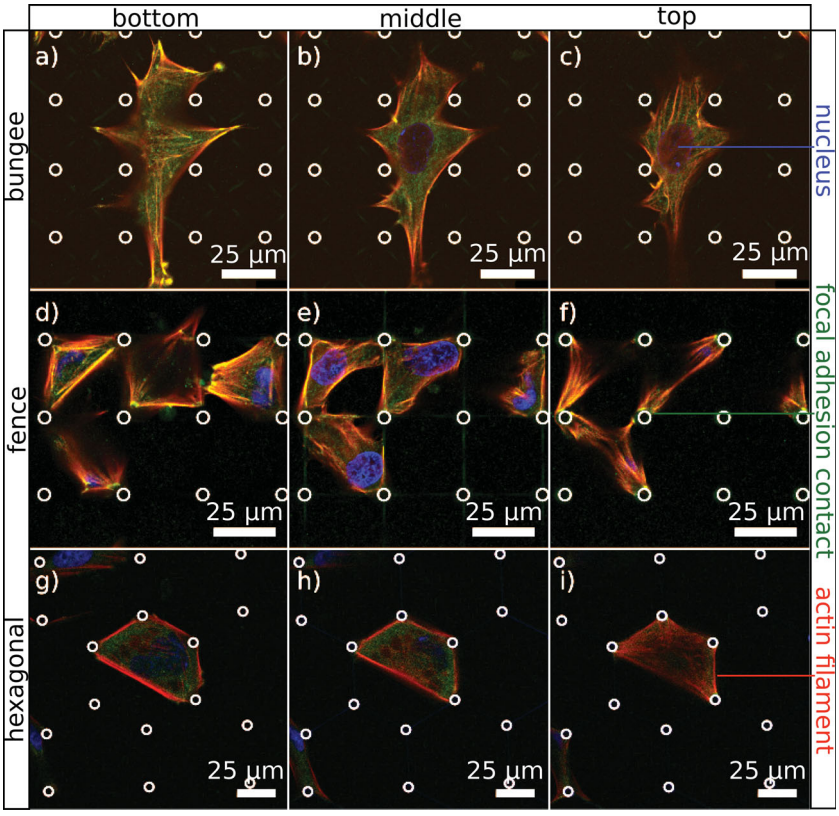

Figure 6. Confocal laser scanning micrographs of fluorescent stained cells on different structures. Actin (red), nucleus (blue) and focal adhesion contacts (green) are dyed. Each column corresponds to a different z-layer of the samples (bottom, middle, top), each row to a different sample (bungee (a–c), fence (d–f), 30 µm hexagonal grid (g–i)). Structures are retraced white as a guide to the eye.

surrounding. Alkaline phosphatase, an osteoblastic marker, is an enzyme involved in the mineralization of bone.[2] Cells possessing alkaline phosphatase appear violet after the staining, thereby we observe that SaOs-2 cells on structured fiels (**Figure 7**b–f) appear darker than cells on plain surfaces (Figure 7a).

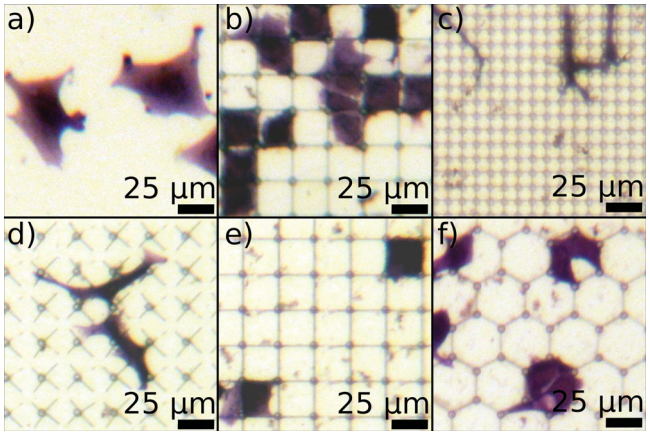

Figure 7. Optical micrographs of SaOs-2 cells (72 h after seeding): Alkaline phosphatase is stained violet and occurs in cells on a) plain surface, b) 25 µm square grid, c) 10 µm square grid, d) bungee, e) fence, f) 25 µm spaced hexagonal grid.

This is not due to the fact that they produce more alkaline phosphate, but a consequence of projection in *x*-*y*-direction. They possess more alkaline phosphatase per *x*-*y*-projection, but not per volume. We observe that alkaline phosphatase is present after 3 and after 6 days both in cells in all structures and in cells on plain surfaces (Figure 7a), ensuring that the structure does not prevent mineralization.

3. Conclusions

We report a systematic study of topographic parameters on osteoblast-like cells. Fabricated structures are chemically identical and possess three-dimensional microfeatures. Since they are coated with titanium dioxide, biocompatibility is ensured. In these topographies, proliferation is enhanced (up to 170%) within 25 µm square grid and hexagonal structures or suppressed (down to 94%) within others compared to unstructured titanium dioxide surfaces (100%). Additionally, we observe a variety of cell morphologies, depending on the three-dimensional surrounding ranging from drawn-out ellipsoids or cells of hexagonal shape to flat and widespread cells. In structures, which influence cells to a three-dimensional growth, a significantly enhanced proliferation is observed. All cells, independently of the topography they grow in, possess alkaline phosphatase, an enzyme that is involved in bone mineralization.

Our experiments show that controlling cell morphology and proliferation via well-defined three-dimensional topographic features is indeed possible. Understanding the important geometrical parameters is crucial and necessary to optimize implant surfaces. However, we are aware of the fact that our study is just the very first step towards this goal. Several technological challenges have to be overcome before these results lead to novel implant surfaces by providing a designer topography that enhances osseointegration.

4. Experimental Section

Preparation of Substrates: Cover slides are used as substrates, since they are suitable for direct laser writing and confocal laser scanning microscopy. The cover slides are cleaned with standard ultrasonic procedure (15 min acetone, 15 min isopropyl alcohol, 15 min ultrapure water) and dried within a nitrogen flow. To enhance adhesion of our photoresist to the glass substrate surface, the cover slides are coated with a self-assembled monolayer (SAM) to which the photo resist can form a covalent bond.[32] To achieve this, substrates are treated with oxygen plasma for 10 min and afterwards placed in a solution of 1 mM 3-methacryloxypropyltrimethoxysilane and toluene for 1 h, rinsed with ultrapure water for 10 min and dried with nitrogen flow.

Photoresist: IP-L 780 (Nanoscribe) is used as photoresist. Since it is acrylate-based it forms a covalent bond to the SAM. One droplet is

placed onto a substrate and directly used for lithography. No pre- or post-bake is necessary.

Direct Laser Writing: Structures are fabricated via direct laser writing, we use a commercially available system (Nanoscribe Photonic Professional). Laser light (wavelength 780 nm, fiber laser) is focused into the photoresist, which is transparent for the fundamental wavelength of the laser. Within the focal volume the resist polymerizes via two photon absorption. When moving the substrate relative to the laser focus nearly arbitrary three-dimensional structures can be produced.[29,32–36] Unexposed areas of photoresist are removed with isopropyl alcohol. Finest feature sizes below 200 nm are possible.[37–39]

Atomic Layer Deposition: Biocompatibility is achieved by coating the structures with titanium dioxide via atomic layer deposition (Picosun R-series atomic layer deposition reactor). We use H_2O and titanium tetraisopropoxide (Picosun) to create a 50 nm thick titanium dioxide layer in anatase phase.

Cell Line: Human osteosarcoma cells (SaOs-2, ATCC HTB-85, kindly provided by Dr. R. Wittig, ILM Ulm) are used for all experiments, because they are able to form a calcifying matrix[40] and reveal the most mature osteoblastic labelling profile compared to MG-63[2,41] and U-2 OS cells.[41] Cells are stored in liquid nitrogen and cultured in Dulbecco's Modified Eagle's Medium (life technologies) containing 10% Fetal Bovine Serum (FBS, Gibco), 100 U/ml penicillin (life technologies), 100 µg/mL streptomycin (life technologies) and 2 mmol/l Glutamax (life technologies) at 37 °C and 5% CO_2. Medium is changed 24 h post melting and afterwards every 3–4 days.

Cell Seeding and Growing: Cells are cultured 5 days in cell culture flasks (Sarstedt) before seeding (day 0) onto the structures with a density of 42 cells/mm^2. To examine proliferation cells are imaged with a microscope (Zeiss PrimoVert) every day and counted afterwards.

Staining Techniques and Imaging: To observe morphology and focal adhesion contacts between cell and substrate, cells are fixed in a solution containing 4% formaldehyde with phosphate buffered saline (PBS, life technologies) 48 h or 72 h post seeding. 48 h post seeding, cells are stained with three fluorescent dyes to observe cell nucleus, actin filament and focal adhesion contacts as described elsewhere.[29] Briefly, cell nucleus is stained using 4′,6-diamidino-2-phenylindole (DAPI, Sigma-Aldrich), actin filament is dyed with phalloidin-tetramethylrhodamine-B-isothiocyanate (phalloidin-TRITC, Sigma- Aldrich) and vinculin is stained using mouse monoclonal anti-vinculin antibody (Abcam) as primary antibody and Alexa-488 goat anti-mouse secondary antibody (life technologies). Staining is performed in a wet and dark chamber to avoid bleaching. 3 or 6 days post seeding alkaline phosphatase is stained using a Sigma alkaline phosphatase staining kit (Sigma, 85L2). Imaging is done with Zeiss Axio Observer LSM 510 and Leica TCS SP5 II and recorded pictures are aligned and cropped with ImageJ.

Statistics: All experiments concerning proliferation are made with at least 12 identical structured fields. Proliferation is measured using the quotient of cell density at 72 h and cell density at 24 h, excluding effects of non-uniform cell seeding. Proliferation graphs show the mean proliferation value of n experiments normalized to the mean value of proliferation on plain surfaces. Error bars indicate standard deviation. Evaluation of significant differences is done with Welch's t-test. Probability values (p-values) are quoted in the graphs, using * for $p < 0.05$, ** for $p < 0.01$, and *** for $p < 0.001$. For $p < 0.05$, the zero hypothesis ("Proliferation is equal on two different surfaces") is rejected and the proliferation within two structures is called significantly different.

Supporting Information

Supporting Information is available from the Wiley Online Library or from the author.

Acknowledgements

The authors thank Prof. Dr. Rudolf Steiner (ILM, Ulm), Dr. Rainer Wittig (ILM, Ulm), and Eva Winkler (ILM, Ulm) for providing the SaOs-2 cells and excellent advice and information on cell culturing, Prof. Dr. Ekkehard Neuhaus (TU Kaiserslautern) and Dr. Torsten Möhlmann (TU Kaiserslautern) for access to their laser scanning microscope, Prof. Dr. Christiane Ziegler (TU Kaiserslautern) for access to her cell culture laboratory and Dr. Thomas Löber (NSC, TU Kaiserslautern) for focused ion beam preparation.

Received: April 29, 2014
Revised: July 4, 2014
Published online: August 25, 2014

[1] P. K. Moy, D. Medina, V. Shetty, T. L. Aghaloo, *Int. J. Oral Maxillof. Impl.* **2005**, *20*, 569.
[2] L. Shapira, A. Halabi, *Clin. Oral Impl. Res.* **2009**, *20*, 50.
[3] L. Postiglione, G. D. Domenico, L. Ramaglia, A. di Lauro, F. D. Meglio, S. Montagnani, *Eur. J. Histochem.* **2009**, *48*, 213.
[4] K. Mustafa, J. Wroblewski, B. S. Lopez, A. Wennerberg, K. Hultenby, K. Arvidson, *Clin. Oral Impl. Res.* **2001**, *12*, 515.
[5] E. Cukierman, R. Pankov, D. R. Stevens, K. M. Yamada, *Science* **2001**, *294*, 1708.
[6] P. Tayalia, C. R. Mendonca, T. Baldacchini, D. J. Mooney, E. Mazur, *Adv. Mater.* **2008**, *20*, 4494.
[7] M. Bigerelle, K. Anselme, *J. Biomed. Mater. Res., Part A* **2005**, *72*, 36.
[8] J. Y. Martin, Z. Schwartz, T. W. Hummert, D. M. Schraub, J. Simpson, J. Lankford, D. D. Dean, D. L. Cochran, B. D. Boyan, *J. Biomed. Mater. Res.* **1995**, *29*, 389.
[9] G. Zhao, A. Raines, M. Wieland, Z. Schwartz, B. Boyan, *Biomaterials* **2007**, *28*, 2821.
[10] L. L. Guehennec, A. Soueidan, P. Layrolle, Y. Amouriq, *Dent. Mater.* **2007**, *23*, 844.
[11] E. Martinez, E. Engel, J. Planell, J. Samitier, *Anat. Anz.* **2009**, *191*, 126.
[12] T. P. Kunzler, T. Drobek, M. Schuler, N. D. Spencer, *Biomaterials* **2007**, *28*, 2175.
[13] K. A. Kilian, B. Bugarija, B. T. Lahn, M. Mrksich, *Proc. Natl. Acad. Sci.* **2010**, *107*, 4872.
[14] S. Ankam, M. Suryana, L. Y. Chan, A. A. K. Moe, B. K. K. Teo, J. B. K. Law, M. P. Sheetz, H. Y. Low, E. K. F. Yim, *Acta Biomater.* **2013**, *9*, 4535.
[15] P. M. Reynolds, R. H. Pedersen, M. O. Riehle, N. Gadegaard, *Small* **2012**, *8*, 2541.
[16] H. V. Unadkat, M. Hulsman, K. Cornelissen, B. J. Papenburg, R. K. Truckenmüller, A. E. Carpenter, M. Wesseling, G. F. Post, M. Uetz, M. J. T. Reinders, D. Stamatialis, C. A van Blitterswijk, J. de Boer, *Proc. Natl. Acad. Sci.* **2011**, *108*, 16565.
[17] M. Ochsner, M. R. Dusseiller, H. M. Grandin, S. Luna-Morris, M. Textor, V. Vogel, M. L. Smith, *Lab Chip, R.Soc.Chem.* **2007**, *7*, 1074.
[18] N. Jain, K. V. Iyer, A. Kumar, G. V. Shivashankar, *Proc. Natl. Acad. Sci.* **2013**, *110*, 11349.
[19] G. G. Reinholz, B. Getz, L. Pederson, E. S. Sanders, M. Subramaniam, J. N. Ingle, T. C. Spelsberg, *Cancer Res.* **2000**, *60*, 6001.
[20] J. O. Gordeladze, C. A. Drevon, U. Syversen, J. E. Reseland, *J. Cell. Biochem.* **2002**, *85*, 825.
[21] M. Bächle, R. J. Kohal, *Clin. Oral Impl. Res.* **2004**, *15*, 683.
[22] E. Eisenbarth, D. Velten, K. Schenk-Meuser, P. Linez, V. Biehl, H. Duschner, J. Breme, H. Hildebrand, *Biomol. Eng.* **2002**, *19*, 243.
[23] I. Grigal, A. Markeev, S. Gudkova, A. Chernikova, A. Mityaev, A. Alekhin, *Appl. Surf. Sci.* **2012**, *258*, 3415.
[24] T. Hirvikorpi, M. Vähä-Nissi, A. Harlin, M. Karppinen, *Thin Solid Films* **2010**, *518*, 5463.

[25] C. S. Chen, M. Mrksich, S. Huang, G. M. Whitesides, D. E. Ingber, *Science* **1997**, *276*, 1425.
[26] M. Théry, A. Pépin, E. Dressaire, Y. Chen, M. Bornens, *Cell Motil. Cytoskeleton* **2006**, *63*, 341.
[27] B. Geiger, J. P. Spatz, A. D. Bershadsky, *Nat. Rev. Mol. Cell Biol.* **2009**, *10*, 27.
[28] K. N. Dahl, A. J. Ribeiro, J. Lammerding, *Circ. Res.* **2008**, *102*, 1307.
[29] R. Wittig, E. Waller, G. von Freymann, R. Steiner, *J. Laser Appl.* **2012**, *24*, 042011.
[30] A. M. Greiner, M. Jäckel, A. C. Scheiwe, D. R. Stamow, T. J. Autenrieth, J. Lahann, C. M. Franz, M. Bastmeyer, *Biomaterials* **2014**, *35*, 611.
[31] D. Hamilton, K. Wong, D. Brunette, *Calcif. Tissue Int.* **2006**, *78*, 314.
[32] F. Klein, B. Richter, T. Striebel, C. M. Franz, G. von Freymann, M. Wegener, M. Bastmeyer, *Adv. Mater.* **2011**, *23*, 1341.
[33] A. M. Greiner, B. Richter, M. Bastmeyer, *Macromol. Biosci.* **2012**, *12*, 1301.
[34] A. Ovsianikov, A. Deiwick, S. Van Vlierberghe, P. Dubruel, L. Moller, G. Drager, B. Chichkov, *Biomacromolecules* **2011**, *12*, 851.
[35] F. Claeyssens, E. A. Hasan, A. Gaidukeviciute, D. S. Achilleos, A. Ranella, C. Reinhardt, A. Ovsianikov, X. Shizhou, C. Fotakis, M. Vamvakaki, B. N. Chichkov, M. Farsari, *Langmuir* **2009**, *25*, 3219.
[36] V. Melissinaki, A. A. Gill, I. Ortega, M. Vamvakaki, A. Ranella, J. W. Haycock, C. Fotakis, M. Farsari, F. Claeyssens, *Biofabrication* **2011**, *3*, 045005.
[37] S. Kawata, H.-B. Sun, T. Tanaka, K. Takada, *Nature* **2001**, *412*, 697698.
[38] M. Deubel, G. von Freymann, M. Wegener, S. Pereira, K. Busch, C. M. Soukoulis, *Nat. Mater.* **2004**, *3*, 444.
[39] J. Fischer, M. Wegener, *Opt. Mater. Express* **2011**, *1*, 614.
[40] S. B. Rodan, Y. Imai, M. A. Thiede, G. Wesolowski, D. Thompson, Z. Bar-Shavit, S. Shull, K. Mann, G. A. Rodan, *Cancer Res.* **1987**, *47*, 4961.
[41] C. Pautke, M. Schieker, T. Tischer, A. Kolk, P. Neth, W. Mutschler, S. Milz, *Anticancer Res.* **2004**, *24*, 3743.